JOURNAL OF CATALYSIS **163,** 12–17 (1996)
ARTICLE NO. 0300

An Atomic Force Microscopy Study of the Morphological Evolution of the MoO_3 (010) Surface during Reduction Reactions

Richard L. Smith and Gregory S. Rohrer*

Department of Materials Science and Engineering, Carnegie Mellon University, Pittsburgh, Pennsylvania 15213-3890

Received January 25, 1996; revised May 13, 1996; accepted May 14, 1996

Atomic force microscopy was used to characterize the nanometer-scale structural evolution of the MoO_3 (010) surface during reaction with hydrogen at 400°C. Two primary surface modifications were identified. First, water vapor, when present in the reactor either as an impurity or as an oxidation product, accelerates the volatilization of MoO_3 and leads to the formation of surface voids. The presence of these voids increases the density of (100) and (h0l)-type surface sites on the basal planes. Second, oxygen removal leads to the formation of crystallographic shear planes. The intersection of these defects with the (010) surface creates 2 Å high steps along ⟨001⟩ and their presence indicates that the surface vacancy concentration has reached an upper limit. The mechanisms by which these structural changes might influence the reactivity of molybdenum oxide catalysts are discussed. © 1996 Academic Press, Inc.

INTRODUCTION

Experimental results have clearly demonstrated that the catalytic properties of certain transition metal oxides depend on the orientation of the bounding surface planes (1–14). However, because the structures of these same surfaces have yet to be described in detail, our mechanistic understanding of this structure sensitivity is limited. A useful description of the surface must specify not only the composition and atomic structure of the termination layer, but also the population and configuration of defects. Steps, point defects, and the intersections of extended defects with the surface can all potentially influence surface properties (15–18). Furthermore, this defect structure is expected to evolve during use of the catalyst. Previous studies of the structural evolution of molybdate and vanadate catalysts have been based on transmission electron microscopy (TEM) observations which typically probe the through-thickness volume of small particles (19, 20). Conventional surface studies of these same materials have been frustrated by their lability; they decompose in vacuum when irradiated by even low-energy electron beams (20–23). Recently developed scanned probe techniques, on the other hand, which include scanning tunneling microscopy (STM) and atomic force microscopy (AFM), are nondestructive and have been used to characterize the structures of even the most fragile surfaces, such as MoO_3 (24) and V_2O_5 (25, 26). The objective of the experiments described in the present paper was to use AFM to determine how the structure of the MoO_3 (010) surface evolves during reduction reactions. The single crystal surfaces were reduced using a H_2–N_2 mixture, with different amounts of water vapor, at 400°C for times ranging between 0.5 and 10 min.

* Author to whom correspondence should be addressed. E-mail: gr20@andrew.cmu.edu; www: http://neon.mems.cmu.edu/rohrer.html.

METHODS

(a) *MoO_3 Crystal Growth*

The single crystals of α-MoO_3 used in these experiments were grown via chemical vapor transport in quartz ampoules. In a typical growth, a quartz tube (I.D. = 13 mm) was charged with 0.09 g/cm^3 of MoO_3 powder (99%, Johnson Matthey) and flamed *in vacuo* to remove residual water. After drying, the tube was vented in a N_2-filled glove bag and 0.004 g/cm^3 of $TeCl_4$ (99.9%, Johnson Matthey) was introduced to act as a transporting agent. The tube was then reevacuated ($P < 4 \times 10^{-5}$ atm) and, finally, sealed to form an ampoule approximately 10 cm in length. The ampoule was then heated in a horizontal tube furnace with the temperature graded from 525 to 500°C along its length. Within five days, transparent, green–yellow crystals with dimensions as large as $5 \times 3 \times 1$ mm could be harvested from the cool end of the tube. Powder X-ray analysis of pulverized single crystals indicated that they were phase pure; all peaks could be indexed unambiguously to an orthorhombic cell in the space group Pbnm. The measured lattice parameters [$a = 3.9664(9)$ Å, $b = 13.8685(30)$ Å, $C = 3.7012(9)$ Å] were refined from 25 peaks and compare favorably with those previously established by Kihlborg (27).

(b) *Surface Reactions*

Single crystals were mounted on a stainless steel disc by spot welding a thin strip of Ta foil across the (010) face.

0021-9517/96 $18.00
Copyright © 1996 by Academic Press, Inc.
All rights of reproduction in any form reserved.

Fresh (010) surfaces were then prepared by cleavage with adhesive tape just prior to insertion of the samples into a quartz reaction tube. The temperature of the reactor was measured by a type K thermocouple located adjacent to the single crystal sample. Initially, the reactant gas was flowed ($P = 1$ atm, flow rate = 200 cc/min) over the sample at room temperature, while a small, horizontal, split-tube furnace was preheated to 400°C. The reaction tube was then lowered into the furnace and the temperature of the sample was monitored. After reacting for a predetermined time at 400°C, the tube was lifted from the furnace and allowed to cool under flowing gas. It took less than 30 s for the samples to reach 400°C during the heat-up period (with the temperature not exceeding 430°C) and less than 1 min for the samples to cool to below 100°C during the cool down.

In the majority of experiments, samples were reacted in as-received forming gas (10% H_2/90% N_2 with 20 ppm H_2O). However, additional experiments were conducted to explore the effect of water vapor in the reactor. Several samples were treated with forming gas that was dried by passing it through columns of $CaSO_4$ and a 4-Å synthetic molecular sieve. Additional samples were treated in N_2 of varying water content (dry, 20 ppm, and saturated with H_2O at 25°C). Finally, several forming-gas-reduced samples were heated in air (in a muffle furnace) at 450°C in an attempt to reoxidize the surface.

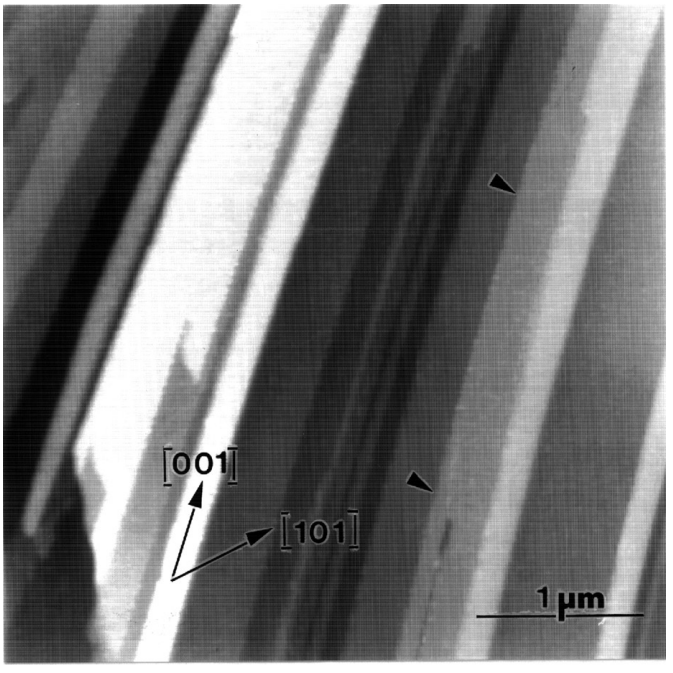

FIG. 1. Topographic AFM image of a freshly cleaved MoO_3 (010) surface. The 4×4 μm area was imaged using a constant force of 2.5 nN. Note the predominance of [001] oriented step edges in this region. A half unit cell height (7 Å) step is indicated by the two arrows.

(c) *AFM Analysis*

Upon cooling to room temperature, samples were removed from the reactor and imaged in the ambient atmosphere with a Park Scientific Instruments scanning probe microscope. The AFM was operated in contact mode (constant force) using pyramidal Si_3N_4 tips and forces between 0.1 and 5 nN. Each sample was imaged for several hours and no changes in surface topography were observed over the analysis period.

RESULTS

A typical AFM image of an α-MoO_3 (010) surface produced by cleavage is shown in Fig. 1. The surface is characterized by atomically flat terraces, often with areas in excess of 200 μm. These terraces are separated by steps or groups of steps with heights that are integer multiples of 7 Å. This distance is 1/2 of the *b* lattice parameter and is, therefore, equal to the distance between the van der Waals gaps that separate adjacent layers of this structure. Throughout the course of study, multiple areas on more than 10 crystals were characterized and steps smaller than 7 Å were never encountered. Though a number of step-edge orientations were observed, the dominant orientation is parallel to [001] and, in many instances, the flat terraces extend without perturbation for more than 1 mm in the [001] direction. As previously reported by Kim and Lieber (24), we found that high resolution images recorded on the terraces have atomic-scale contrast which reflects the pattern of MoO_6 octahedral groups that are expected to terminate this surface.

Reduction at 400°C in forming gas causes two distinct changes in the structure of the (010) surface. First, small steps oriented parallel to [001] are found on the surface within the first 30 s of the reaction. The steps have an irregular spacing and, as shown in Fig. 2, they appear as a streaky contrast along the [001] axis. The height of these steps is smaller than any step ever observed on the untreated surface; it is approximately 2 Å. The second change is that voids (pits) form on the previously flat surface. The pits have widths on the order of 800 Å and depths of 20 Å and some examples are shown in Fig. 3. After surveying many areas, it was apparent that the pits form with equal probability on both the terraces and step–edges.

Surfaces reacted for longer periods of time show similar features. However, with increasing reaction time, the number and size of the surface voids increase (see Fig. 4). Within the first 5 min of reaction, voids as large as 1 μm in diameter and 200 Å in depth were observed. After 10 minutes, some surface voids grew to the point that they coalesced with others. While the pits are not completely faceted, many of their bounding edges display a preferential orientation. The preferred orientation appears to be along directions near ⟨101⟩, as shown in Fig. 5. They are, however, not exactly aligned along this low index direction; their orientation axis

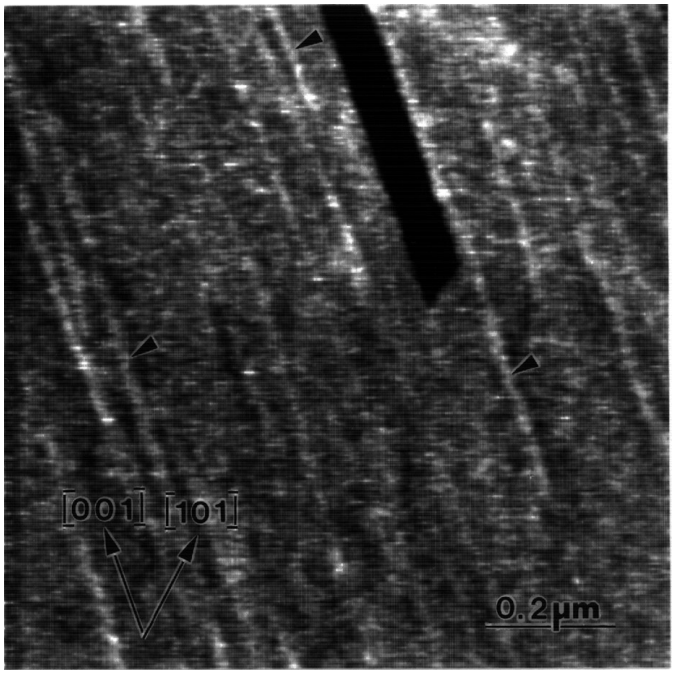

FIG. 2. Topographic AFM image of a MoO_3 (010) surface after reaction with 10% H_2–N_2 (with 20 ppm H_2O) for 2 min at 400°C. For clarity, several of the small (2 Å) surface steps are indicated by arrows.

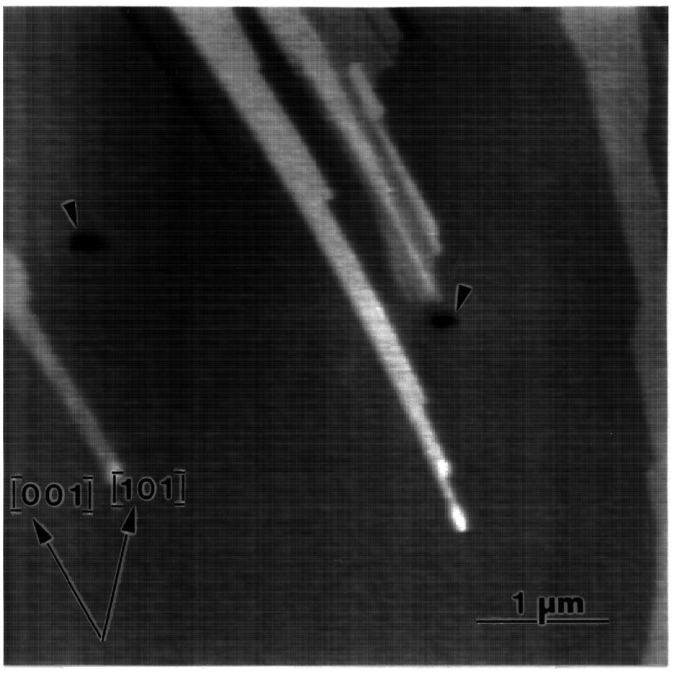

FIG. 3. Topographic AFM image of a MoO_3 (010) surface after reaction with 10% H_2–N_2 (with 20 ppm H_2O) for 30s at 400°C. Two small surface voids (the black contrast indicated by the arrows) are visible on the flat terrace.

typically intersects [001] at angles of 51 and 35° rather than the expected angle of 43°. Finally, we note that for all but the longest reaction times, the crystals were visually unaffected by the treatments. Only after 10 min of reaction did the crystals begin to take on the blue-gray color that is characteristic of substoichiometric molybdenum trioxide.

While the changes described above were characteristic of all samples reacted in forming gas, crystals treated in dried mixtures were found to have considerably fewer (and smaller) voids than those heated in undried mixtures for equivalent durations. To separate the effects of water produced by the reaction of H_2 with the crystal and water present as an impurity in the gas stream, a subset of samples were treated in flowing N_2 containing known amounts of water vapor. Surfaces treated in dried N_2 showed no indications of pitting, even after treatments in excess of 5 min. However, the presence of just 20 ppm H_2O resulted in the formation of surface voids similar to those found on the samples treated in forming gas. Crystals treated in N_2 which was saturated with H_2O at 25°C displayed accelerated pitting. Within 5 minutes at 400°C, a severely stepped, cellular structure developed on the surface (see Fig. 6); the step edges are preferentially oriented (much like the void edges) nearly parallel to the ⟨101⟩ directions.

To test reversibility, one crystal was reduced for 2 min in forming gas at 400°C, and then heated in air at 450°C for 5 min. Betweem treatments, the (010) surface was analyzed with AFM and characteristic structural features were noted. Upon returning to the same areas, after the oxidation treat-

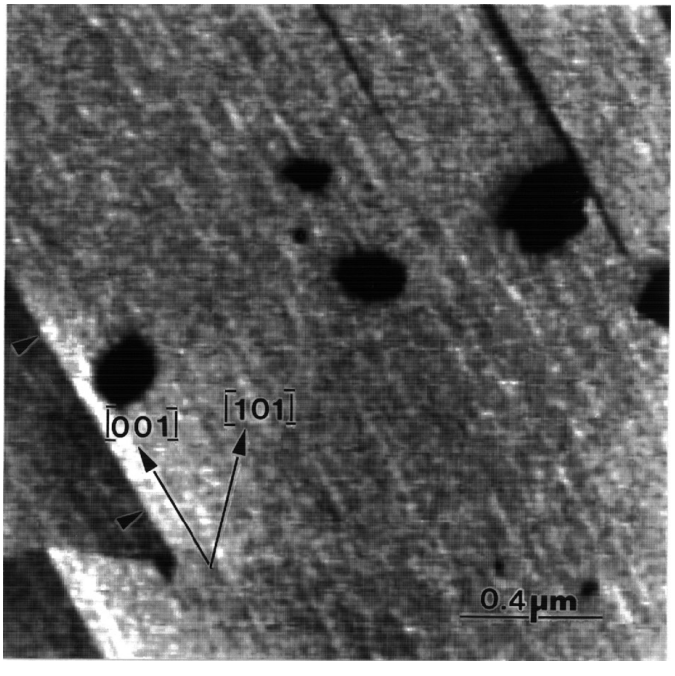

FIG. 4. Topographic AFM image of a MoO_3 (010) surface which has reacted with 10% H_2–N_2 (with 20 ppm H_2O) for 2 min. In this $1.9 \times 1.9\ \mu$m image, the surface voids, a 7-Å step (indicated with arrows), and the 2-Å surface steps (the streaky contrast parallel to [001]) are all distinguished.

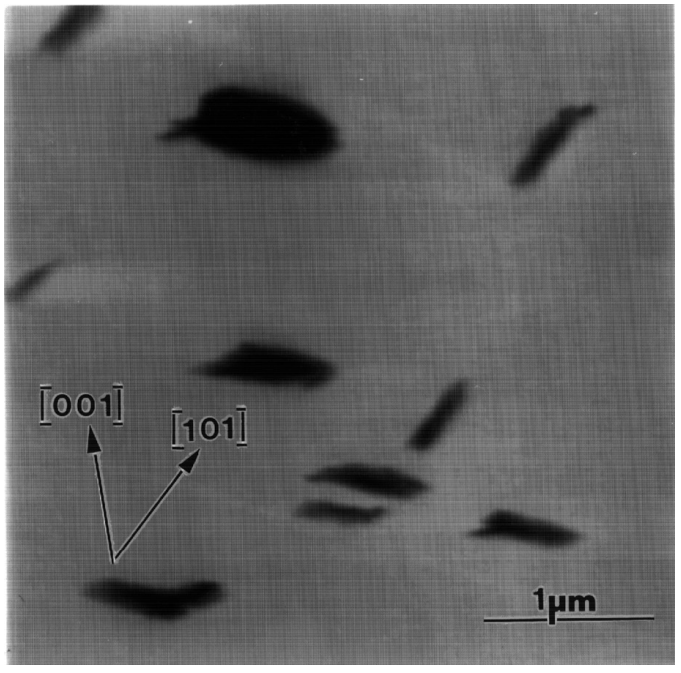

FIG. 5. Topographic AFM image of a MoO_3 (010) surface after treatment for 5 min at 400°C in 10% H_2–N_2 (with 20 ppm H_2O). Note the orientational order and high aspect ratio of the surface voids (black contrast) in this 4×4 μm image.

ment no change in the size or shape of the surface voids was evident. Additionally, the small surface steps were found to persist through the treatment.

DISCUSSION

Based on the results of the experiments described above, the structure of the MoO_3 surface is modified during the reduction process, especially in the presence of water vapor. Surface voids form in less than 30 s and increase in size and density as the reaction time and/or water content increases. The series of N_2 treatments clearly shows that water vapor is necessary for void nucleation and growth at 400°C. If the gas is dried prior to reaction and no water vapor is formed during the treatment, then no voids are found on the sample, even after treatments in excess of 5 min. The simplest explanation for the pit formation is that the MoO_3 (010) surface is subliming at the reaction temperature. The observation that water vapor accelerates the sublimation process is not surprising. It has long been known that H_2O can be used as a mineralizing agent in the chemical vapor transport synthesis of oxide single crystals (28). During these reactions, transport is enhanced by the formation of gaseous hydroxides or oxy-hydroxides. The likely pitting mechanism involves the formation and evaporation of molybdenum oxy-hydroxide species (such as $MoO_2(OH)_2$) at the surface.

It is unclear whether or not preferential nucleation sites for voiding exist at the interface. While no heterogeneity has been identified on the fresh cleaved surface and the pits appear to be distributed randomly, it is possible that nucleation sites form while the crystal is being heated to the reaction temperature. Several investigators (19, 20) have reported the formation and growth of oxygen deficient domains when MoO_3 is reduced at temperatures below 300°C. The domain boundaries are oriented parallel to ⟨304⟩ (very near ⟨101⟩) and the lattice within the domain is displaced from that of the matrix by a shear vector $\mathbf{b} \approx 1/2\,[101]$ across the boundary (19). It is interesting to note that, within experimental error, the pits have the same orientation as the oxygen deficient domains. This prompts speculation that the domains or the domain boundaries provide heterogeneous nucleation sites for the voids, a plausible argument considering the strain that is expected in the vicinity of the domain boundary and in the oxygen deficient domain. The observation of similar voiding in humid N_2 environments might be explained by the same phenomenon since the partial pressure of O_2 is also very low under these conditions.

Because some water is always present, at least as a deep oxidation product, we assume that the pit formation process occurs under a wide variety of reaction conditions. Furthermore, the morphological changes associated with this process probably influence the properties of MoO_3 catalysts. Studies on the reactivity of highly oriented MoO_3 catalysts have shown that the basal facets (the {010} surfaces) favor the deep oxidation of feedstocks such as methane and 1-butene (14) while the side planes (the {100} and {h0l}

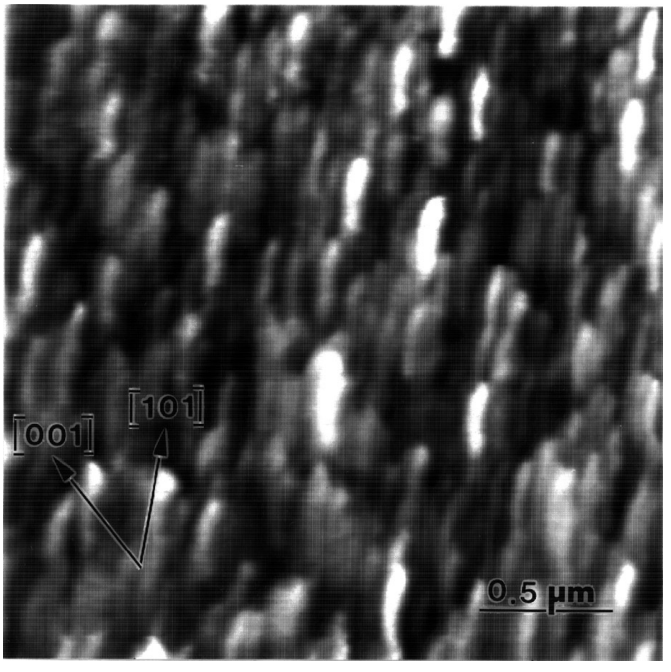

FIG. 6. Topographic AFM image of a MoO_3 (010) surface which was treated for 5 min at 400°C in N_2 which was saturated with water vapor at 25°C. The steps are nearly parallel to ⟨101⟩, an orientation rarely seen on fresh cleaved surfaces.

surfaces) show a higher selectivity to partial oxidation products. Furthermore, studies of the conversion of propene to acrolein indicate that this oxidation reaction proceeds via a two-step process which requires sites on both the side and the basal planes to be in close proximity, (8). If we accept these mechanisms, our results indicate that the pits which form on the basal facets, after exposure to water vapor, might enhance the ability of MoO_3 to catalyze some partial oxidation reactions. Pitting increases the number of side plane sites and brings more basal plane sites and side plane sites into close proximity. It is interesting to note that while the initial powder morphology of a catalyst may favor deep oxidation products (i.e., be highly oriented to {010}), one of these products (H_2O) will cause the catalyst to evolve toward a morphology with greater selectivity to partial oxidation products. Finally, we should mention that pitting does not occur when samples are treated at or below 300°C. This observation might explain why the MoO_3 (010) surface is inactive for methanol oxidation at lower temperatures (7).

Molybdenum trioxide is one of a number of transition metal oxides that accommodate oxygen deficiency through the formation of oxygen vacancies and crystallographic shear (CS) planes (20). When the shear vector of a CS plane has a component that is normal to the surface plane, a small step must be created along the CS plane/surface intersection. Both TEM and LEED studies have revealed that when MoO_3 is reduced, CS planes form along [001] and have a shear vector of $\mathbf{b} = (a/2, b/7, 0)$ (19, 20). Thus, the 2 Å ($\sim b/7$) steps that are found on the reduced MoO_3 (010) surface are easily explained as the intersection of CS planes with the surface. This shear vector is parallel to the edge of an MoO_6 octahedron in the structure and is, therefore, common to a number of the so-called "CS phases" in the binary Mo–O system (20, 27). $Mo_{18}O_{52}$ is one such phase and a STM study of the (100) surface of this compound has confirmed the existence of a small step at the CS plane/surface intersection (29).

The formation of CS planes at the MoO_3 (010) surface introduces a number of changes that might influence its catalytic properties. For example, new atomic coordination environments occur where MoO_6 octahedra share edges at the CS plane/surface intersection (15, 20, 27). Also, the CS planes form only after the surface is supersaturated with oxygen vacancies and, thus, they act as sinks for the point defects. The CS planes grow into the bulk by the climb of bounding partial dislocations and, therefore, they consume oxygen vacancies and sites as they extend into the interior of the crystal. The presence of CS planes in our samples indicates that at 400°C, in the presence of H_2, the equilibrium concentration of surface vacancies has already reached its upper limit. This observation is consistent with earlier TEM studies (19). If oxygen vacancies are assumed to be preferred reaction sites, then CS plane formation will limit the catalyst's activity. If, on the other hand, CS planes enhance partial oxidation processes, as suggested by Broclawik and Haber (15), then the reverse might be true. Finally, it is important to realize that CS planes affect both the mass and charge transport properties of the oxide. For example, O'Keeffe (30) has pointed out that CS planes might provide high diffusivity pathways for oxygen ions. Furthermore, it is known that as the oxygen deficiency and CS plane density increases, the electronic conductivity of the oxide also increases (31).

A number of authors have experimentally explored the influence of CS planes on the catalytic properties of several Mo–O phases (16, 17). While the results clearly demonstrate that the presence of CS planes influences the catalytic properties of chemically similar oxides, the mechanisms at work remain obscure.

The results of our preliminary reoxidation experiments suggest that reduction in forming gas proceeds more quickly than oxidation in air. Both the surface voids and CS planes persisted during heating in air. Based on the proposed sublimation mechanism, the stability of the surface voids is certainly expected. However, the persistence of the CS planes is not as easily explained. The surface step will be annihilated only when the CS plane climbs out of the crystal. This non-conservative process requires oxygen vacancies to diffuse from the line where the CS plane ends in the bulk to the surface where they are consumed by oxygen adatoms. This is the reverse of the CS plane formation process, where oxygen vacancies are created at the surface and then diffuse to the end of the defect plane. Assuming that oxygen is transported by the same mechanism in both cases, the slower oxidation kinetics could be explained if the oxygen chemical potential gradient is smaller during the reoxidation experiment than it was during the reduction experiment. We expect that further studies of the oxidation behavior will clarify this issue.

ACKNOWLEDGMENTS

This work was supported by the National Science Foundation under YIA Grant DMR-9458005. Helpful comments from Professor H. Kung of Northwestern University are greatly appreciated.

REFERENCES

1. Tatibouët, J. M., and Germain, J. E., *J. Catal.* **72**, 375 (1981).
2. Volta, J. C., and Tatibouët, J. M., *J. Catal.* **93**, 467 (1985).
3. Haber, J., *in* "Solid State Chemistry in Catalysis" (R. Grasselli and J. Brazdil, Eds.), p. 1. American Chemical Society, Washington, D.C., 1985.
4. Germain, J. E., *in* "Adsorption and Catalysis on Oxide Surfaces" (M. Che and G. C. Bond, Eds.), p. 355. Elsevier, Amsterdam, 1985.
5. Tatibouët, J. M., Phichitkul, Ch., and Germain, J. E., *J. Catal.* **99**, 231 (1986).
6. Ziolkowski, J., *J. Catal.* **100**, 45 (1986).
7. Farneth, W. E., McCarron, E. M., III, Sleight, A. W., and Staley, R. H., *Langmuir* **3**, 217 (1987).
8. Brückman, K., Grabowski, R., Haber, J., Mazurkiewicz, A., Sloczynski, J., and Wiltowski, T., *J. Catal.* **104**, 71 (1987).

9. Brückman, K., Haber, J., and Wiltowski, T., *J. Catal.* **106**, 188 (1987).
10. Anderssen, A., and Hansen, S., *J. Catal.* **114**, 332 (1988).
11. Mingot, B., Floquet, N., Bertrand, O., Treilleux, M., Heizmann, J. J., Massardier, J., and Abon, M., *J. Catal*, **118**, 424 (1989).
12. Abon, M., Massardier, J., Mingot, B., Volta, J. C., Floquet, N., and Bertrand, O., *J. Catal.* **134**, 542 (1992).
13. Guerrero-Ruiz, A., Blanco, J. M., Aguilar, M., Rodriguez-Ramos, I., and Fierro, J. L. G., *J. Catal.* **137**, 429 (1992).
14. Smith, M. R., and Ozkan, U. S., *J. Catal.* **141**, 124 (1993).
15. Broclawik, E., and Haber, J., *J. Catal.* **72**, 379 (1981).
16. Barber, S., Booth, J., Pyke, D. R., Reid, R., and Tilley, R. J. D., *J. Catal.* **77**, 180 (1982).
17. McCormick, R. L., and Schrader, G. L., *J. Catal.* **113**, 529 (1988).
18. Wandelt, K., *Surf. Sci.* **251/252**, 387 (1991).
19. Gai-Boyes, P. L., *Catal. Rev.-Sci. Eng.* **34**, 1 (1992).
20. Hyde, B. G., and Bursill, L. A., *in* "The Chemistry of Extended Defects in Nonmetallic Solids" (L. Eyring and M. O'Keeffe, Eds.), p. 347. North-Holland, Amsterdam, 1970.
21. Colpaert, M. N., Clauws, P., Fiermans, L., and Vennik, J., *Surf. Sci.* **36**, 513, (1973).
22. Firment, L. E., and Ferretti, A., *Surf. Sci.* **129**, 155 (1983).
23. Dufour, L. C., Bertrand, O., and Floquet, N., *Surf. Sci*, **147**, 396 (1984).
24. Kim, Y., and Lieber, C. M., *Science* **257**, 375 (1992).
25. Oshio, T., Sakai, Y., and Ehara, S., *J. Vac. Sci. Technol. B* **12**, 2055 (1994).
26. Smith, R. L., Lu, W., and Rohrer, G. S., *Surf. Sci.* **322**, 293 (1995).
27. Kihlborg, L., *Arkiv Kemi* **21**, 471 (1963).
28. Schäfer, H., "Chemical Transport Reactions," Academic Press, New York, 1964.
29. Rohrer, G. S., Lu, W., Smith, R. L., and Hutchinson, A., *Surf. Sci.* **292**, 261 (1993).
30. O'Keeffe, M., *in* "Fast Ion Transport in Solids, Solid State Batteries, and Devices" (W. Van Gool, Ed.), Proceedings of the NATO Advanced Study Institute, p. 233. North-Holland, Amsterdam, 1973.
31. Greenblatt, M., *Chem. Rev.* **88**, 31 (1988).